
LMECA2323 - Turbomachinery

Project – 2023

Characterization of a high-pressure turbine stage
for an industrial power production gas turbine

Professors

L. Bricteux
S. Lavagnoli

Teaching Assistants

Ir. Romain Debroyer
Ir. Antoine Verhaeghe

Student:

SANGHVI, Mahek Atul (NOMA: 15412201)

TABLE OF CONTENTS

1. Introduction	6
2. 1d Mean Line Design	7
2.1 Input Data.....	7
2.2 Design Procedure	8
2.2.1 Inlet Condition Calculations	8
2.2.2 Required P3 Calculations	10
2.2.3 Assumptions Of Design Parameters	11
2.3 Thermodynamic Quantities	12
2.3.1 Station 2 Stator Calculations	13
2.3.2 Relative Rotor Inlet Condition	14
2.3.3 Rotor Outlet	15
2.3.4 Comparison Of Enthalpy	16
2.4 Velocity Triangles.....	19
2.5 H-S Diagram	20
2.6 Annulus Sizing	21
2.7 Design Constraints	23
3. Rotor Blade Design	24
3.1 Input Data Assumptions	24
3.2 Design Procedure & Calculations	25
3.3 Main Blade Parameters	26
4. Rotor Blade Construction And Cfd Evaluation	28
4.1 Blade Passage Geometry	28

4.2	Evaluation Of Profile Curvature And Passage Area.....	28
4.3	Cfd Evaluation.....	29
4.3.1	Mesh Generation.....	29
4.3.2	Cfd Setting.....	30
4.3.3	Cfd Convergence	31
4.4	Isentropic Static Pressure Distribution.....	31
4.5	Colourmaps Of Cfd Analysis	32
4.6	Velocity Profile Highlight The Momentum Deficit In Wake	34
4.7	Cfd Prediction Result:	34
5.	Conclusion	36

TABLE OF FIGURES

Fig. 1: Siemens SGT5-4000f Core Engine	6
Fig. 2: Stations Of 1st Stage Of Turbine.....	8
Fig. 3: Comparison Of Enthalpy For Approval Of Design.....	17
Fig. 4: Velocity Triangle For Both Station 2 And 3	19
Fig. 6: Stagger Angle Correlation [Kacker And Okapuu, 1982].....	24
Fig. 7 Blade Profile Diagram	28
Fig. 8 Blade Passage Area Variation	28
Fig. 9: Blade Thickness Variation Along U	29
Fig. 10: Curvature K Along U	29
Fig. 11: Cascading View Of Turbine Rotor Blades Of Stage 1	29
Fig. 12: Blade Profile Generated Using Gmsh	30
Fig. 13: Cauchy Cd Convergence	31
Fig. 14: Static Pressure Variation Along The Blade.....	32
Fig. 15: Mach Variation Along The Blade	33
Fig. 16: Pressure Variation Along The Blade.....	33
Fig. 17: Specific Enthalpy Variation.....	33
Fig. 18: Entropy Variation	33
Fig. 19: Momentum Variation In The Wake	34
Fig. 21: Mach Distribution Along The Pitch	35

LIST OF TABLES

Table 1: Iterations For Various Properties And For Different Assumed Values	17
Table 2: Velocity Triangle Parameters Data.....	19
Table 3: Enthalpy-Entropy Results Table	20
Table 4: Comparison Of Design Control Parameters And Obtained Results	23
Table 5: Main Blade Parameters	26
Table 6: SU2 CFD Solver Configuration Data	30

1. INTRODUCTION

Turbomachine deals with production of energy by change of enthalpy for a continuous flowing stream and transfer work through a shaft. This work production is done by the turbine from the combustion of fuels. The turbine works on the principle of expansion. Expansion occurs by increase in velocity at the cost of pressure. The majority is consumed by the compressor which is transferred through shaft.

The designing of turbine deals with various thermodynamic properties, annulus sizing and much more. The process of designing involves

- 1-D Mean Design
- Rotor Blade Design
- CFD simulation of the blade

These are basic design procedure for a design engineer. But this process doesn't go simultaneously. We have to iterate till we reach the design guidelines as mentioned. Iteration involves parameter iteration, design iteration and design step iteration.

This design of turbine blades focusses on high pressure turbine with four stages. The focus is on 1st stage of the turbine for the SGT5-4000F engine.

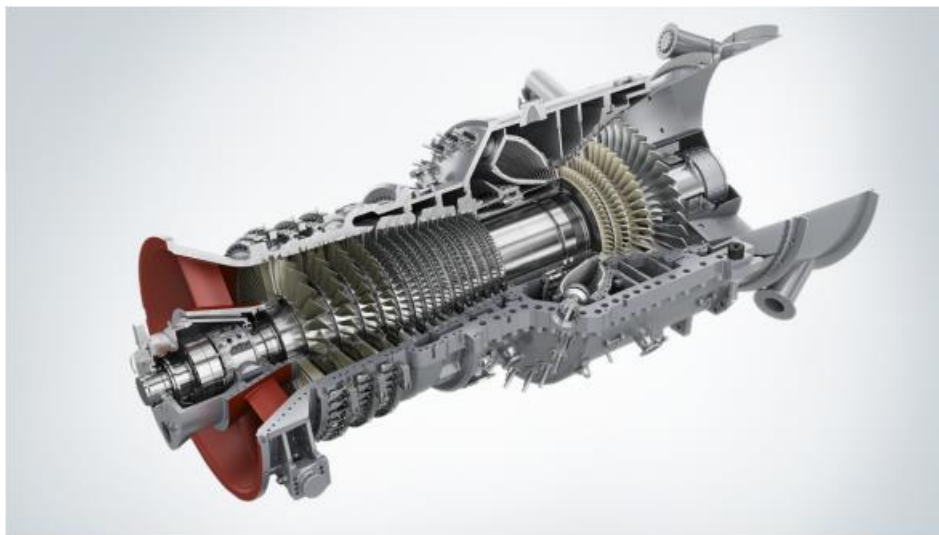


Fig. 1: Siemens SGT5-4000F core engine

2. 1D MEAN LINE DESIGN

A simplified modelling strategy utilized in the early stages of turbine design is referred to as 1D mean turbine design. It entails utilizing mathematical models and simplified assumptions to evaluate a turbine's performance and attributes using one-dimensional (1D) analysis.

In a 1D mean design, the axial symmetry of the flow through the turbine is assumed, and the flow is averaged along the radial direction. Engineers can quickly calculate critical factors like turbine power output, efficiency, and blade loading thanks to this simplification.

2.1 INPUT DATA

During design various inputs are provided to start the computation of parameters and assumption of parameters to design the turbine.

The following parameters are provided:

- The working fluid is a calorifically perfect diatomic gas with the following properties:
 - the ratio of specific heat, $\gamma = 4.0/3.0$,
 - the specific gas constant $R = 287 \text{ Jkg}^{-1}\text{K}^{-1}$
- Turbine mass flow rate $m = 750 \text{ kg/s}$, the fuel-air ratio for a heavy-duty industrial gas turbine is $f_{ar} = 0.025$.
- Turbine stage (extracted) power at the shaft $P = 330 \text{ MW}$. Recall that the turbine also drives the compressor which has to be taken into account in the power budget.
- Overall static pressure ratio for the compressor $\Pi_C = 20$.
- Compressor admission static conditions $T_{adm} = 15^\circ\text{C}$ and $P_{adm} = 101325 \text{ Pa}$.
- Compressor isentropic efficiency $\eta_{sic} = 0.92$.
- Mach number in the combustion chamber $M_{comb} = 0.15$.
- Turbine inlet static temperature for an F-class turbine $TIT = 1400^\circ\text{C}$
- Turbine inlet yaw angle $\alpha_1 = 0^\circ$ (fully axial)

- As the shaft is connected to a synchronous generator the rotational speed is $N_{\text{rot}} = 3000$ rpm.
- Due to centrifugal stress limitations, the blade peripheral velocity is limited such that at the mean radius $U_m = \omega \times R_m = 350$ m/s.
- In order to ensure a safe and realizable turbine, your design must respect the general mechanical design constraint that AN2 value must be lower than $3\text{E} + 07 \text{ m}^2\text{rpm}^2$

In your design process, you must make the following assumptions:

- The mean-line radius R_{mean} does not change across the turbine stage, and its value is given as input data,
- The blading efficiencies of both stator and rotor rows are to remain fixed throughout your 1D design at the value of $\eta_{\text{S,R}} = 0.90$

2.2 DESIGN PROCEDURE

A systematic approach with various assumptions and iterations the design of a 1-D mean design is carried out. The the stage of turbine is divide into 3 stations as shown in Fig. 2. The turbine has 4 stages but we focus on single stage. A single stage of turbine has a set of stator and rotors. And each position is given a naming to find the parameters at that point.

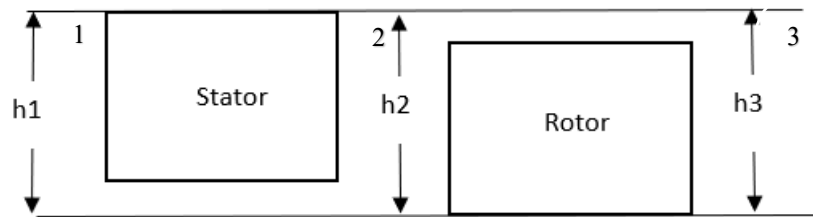


Fig. 2: Stations of 1st stage of turbine

The calculations start with isentropic relations considering no losses in the transfer of energy. So, it starts with amount of enthalpy change is required from a single stage of an axial turbine of high-pressure type for the given turbomachine.

2.2.1 INLET CONDITION CALCULATIONS

The inlet conditions need to be calculated from the compressor details to be used for turbine inlet based on some assumptions.

The specific constants at constant pressure are not given as an input parameter but using the Eq. 1 and Eq. 2 we compute the values for c_p and c_v .

$$c_p = \frac{\gamma R}{\gamma - 1} = 1156.69 \rightarrow (1)$$

$$c_v = \frac{R}{\gamma - 1} = 869.69 \rightarrow (2)$$

The ratio of specific heat ratio for compressor is 1.4 and not the given specific heat ratio as only air passes through the compressor and not the air and fuel mixture.

Firstly, the mass flow rate is different from the turbine than compressor because of only air flows into the compressor.

The formula deduced for calculating mass flow of compressor is found in Eq. 3.

$$m_c = \frac{\dot{m}_T}{1.025} = 731.707 \text{ kg/s} \rightarrow (3)$$

Then to compute the power utilised by the compressor is performed by Eq. 4.

$$P_c = \frac{1}{\eta_{iss}\eta_m} \dot{m} \left(\frac{\gamma}{\gamma - 1} \right) R T_1 \left[\left(\frac{P_2}{P_1} \right)^{\frac{\gamma-1}{\gamma}} - 1 \right] = 327.8 \text{ MW} \rightarrow (4)$$

The mechanical efficiency assumed is 0.95 and efficiency of compressor is given as 0.92. The assumption made is just mention that some amount of energy is lost due to energy transfer through shaft.

And finally, we require intake pressure values which can be computed from exit pressure of the compressor. We neglect any losses for static pressure transferred from compressor to combustion chamber to finally turbine.

Using Eq. (5) we solve for exit static pressure.

$$P_{exit} = \Pi_c \times P_{adm} = 20 \times 101325 = 2026500 \text{ Pa} \rightarrow (5)$$

$$\Rightarrow P_{exit} = P_1$$

The inlet static pressure and static temperature are known but the stagnation properties are unknown which can be found using the isentropic relations in Eq. 6 and Eq. 7 respectively.

$$P_{01} = P_1 \left(1 + \frac{\gamma - 1}{2} M_{cc}^2 \right)^{\frac{\gamma}{\gamma - 1}} = 2056992.5 \text{ Pa} \rightarrow (6)$$

$$T_{01} = T_1 \left(1 + \frac{\gamma - 1}{2} M_{cc}^2 \right) = 1679.21 \text{ K} \rightarrow (7)$$

In this case, $T_1 = TIT$ which is the turbine inlet temperature and M_{cc} is the Mach number exiting the combustion chamber. Using these values, we are capable of computing P_3 .

2.2.2 REQUIRED P3 CALCULATIONS

The turbine expansion needs to be computed to assume the Mach at station 3. So, computation of expansion is done by the following steps.

$$\Delta H_{T,real} = \frac{P}{\dot{m}} = 219.2 \text{ kJ/s} \rightarrow (8)$$

The Eq. 8 gives the enthalpy change required based on the power and mass flow rate in the turbine. The Power is computed as in Eq. 9.

$$P = (P_c + P_T)/4 = 164.45 \text{ MW} \rightarrow (9)$$

Assuming the total-to-total efficiency as 0.87 we obtain the isentropic enthalpy change as in Eq. 10.

$$\Delta H_{T,is} = \frac{\Delta H_{T,real}}{\eta_{TT}} = 243.64 \text{ kJ/s} \rightarrow (10)$$

And from the enthalpy change the isentropic exit stagnation temperature and stagnation pressure is found using the Eq. 11 and Eq. 12 respectively.

$$T_{03is} = T_{01} - \frac{\Delta H_{T,is}}{c_p} = 1468.57 \text{ K} \rightarrow (11)$$

$$P_{03} = P_{01} \left(\frac{T_{03is}}{T_{01}} \right)^{\frac{\gamma}{\gamma - 1}} = 1198493.19 \text{ Pa} \rightarrow (12)$$

And finally, the expansion in the first stage of high-pressure turbine is found using the Eq. 13.

$$\Pi_{TT,is} = \frac{P_{03is}}{P_{01}} \approx 2 \rightarrow (13)$$

Based on this expansion we assume the exit Mach number $M_3=0.3$ which should be between 0.3-0.4.

Using this M_3 , the computation of P_3 is performed with set of equations from Eq. 14 to Eq.17.

$$a_3 = \sqrt{\gamma R T_{01,is}} = 748.71 m/s \rightarrow (14)$$

$$V_{3,is} = a_3 M_3 = 224.61 m/s \rightarrow (15)$$

$$T_{3is} = T_{03is} - \frac{V_{3is}^2}{2c_p} = 1446.77 K \rightarrow (16)$$

$$P_3 = P_{03} \left(\frac{T_{3is}}{T_{03is}} \right)^{\frac{\gamma}{\gamma-1}} = 1107264.59 Pa \rightarrow (17)$$

In these equation a_3 computes the speed of sound at station 3 and V_{3is} computes the absolute velocity at station 3 isentropic. Finally, P_3 is obtained which is used to compute further calculations but it is obtained in isentropic conditions.

2.2.3 ASSUMPTIONS OF DESIGN PARAMETERS

The 3 main parameters to decide and iterate to get optimized results based on design criteria are flow coefficient ϕ , stage loading ψ and Degree of reaction.

Based on the condition that engine is high pressure turbine and expansion is around 2 we assume these quantities and later to get optimized results based on design criteria set we manipulate the coefficients.

1. Stage loading (ψ):

Stage loading controls the relative width of velocity triangles. The stage loading for high pressure is typically fixed between 1.5 to 2. Stage loading effects the turning angle, the exit Mach number and stages as well. As we increase the stage loading the turning angle is higher and exit Mach number is higher with less stages. Whereas, if the stage loading decreases it implies the larger wetted area which implies more stages is required to generate the required amount of power.

We have to control the stage loading such that it does not exceed the blade mean speed which is 350m/s in this engine which is given parameter. The relation between stage loading and blade speed is given by Eq. 18.

$$\psi = \frac{\Delta H_{T,real}}{U^2} \rightarrow (18)$$

Assuming stage loading as 1.8 we compute the blade speed and it is found to be around 350m/s. Also, by observing we can say that stage loading cannot be decreased as the blade mean speed will be higher than 350m/s.

$$U_m = \sqrt{\frac{\Delta H_{T,real}}{\psi}} = 349.02m/s \rightarrow (19)$$

2. Flow Coefficient (ϕ):

Flow coefficient represents the height of the velocity triangles to the length of the blade mean speed. With higher flow coefficient the exit Mach number increases but also the number of blades increases. The change in beta, flow angle decreases with this increase in flow coefficient.

We compute this using smith chart by fixing an efficiency and ψ value we locate the flow coefficient and is found that ϕ is 0.5. Generally, it is found by using the Eq. 20.

$$\phi = \frac{V_x}{U} = 0.5 \rightarrow (20)$$

3. Degree of Reaction (r):

Degree of reaction decides the amount of work done by the stator and rotor of a stage. It mathematically defined as a ratio of enthalpy change in rotor to stage as described in Eq. 21. For lower degree of reaction inlet stagnation pressure and temperature decreases, decrease in axial thrust is also observed. But in the contrary, it leads to easier colling and lower leakage of pressure.

For aircraft application the degree of reaction is around 0.5 but for high pressure turbine cooling is a major factor so the range varies from 0.35 – 0.5. Degree of reaction is assumed to be 0.35.

$$r = \frac{h_3 - h_2}{h_3 - h_1} = \frac{P_2 - P_3}{P_1 - P_3} = 0.35 \rightarrow (21)$$

2.3 THERMODYNAMIC QUANTITIES

The inlet pressure and temperature are known as well as the assumed parameters such as exit Mach number, flow coefficient, stage loading and degree of reaction and from these we also have assumed exit static pressure P_3 . Now with these values we compute the thermodynamic

properties at stage 2 and stage 3. The final destination to create a change in enthalpy which can be equated to the change in enthalpy calculated from power and mass flow rate from Eq. 8. To compare this and reach at good P_3 value we create a loop and use Newton Raphson's method to reach the required enthalpy change. The results for all iterations have been tabulated in table 1.

2.3.1 STATION 2 STATOR CALCULATIONS

At station 2 we have exit of stator from the parameters we calculated the axial component of absolute velocity from Eq. 22. And also, we are aware of degree of reaction so we can compute P_2 from definition of degree of reaction as in Eq. 23.

$$V_{x2} = U_m \phi \rightarrow (22)$$

$$P_2 = r \times (P_1 - P_3) + P_3 \rightarrow (23)$$

Consideration of isentropic expansion is considered and absolute velocity is computed using Eq. 24. And using Eq. 25 computation of static temperature is made.

$$V_{2is} = \sqrt{2c_p T_{01} \left(1 - \left(\frac{P_2}{P_1} \right)^{\frac{\gamma-1}{\gamma}} \right)} \rightarrow (24)$$

$$T_{2is} = T_{01} - \left(\frac{V_{2is}^2}{2c_p} \right) \rightarrow (25)$$

Considering efficiency of stator which is given we find real absolute velocity using Eq. 26. And using this velocity the actual static temperature is computed as in Eq. 27.

$$V_2 = \sqrt{\eta_s \times V_{2is}^2} \rightarrow (26)$$

$$T_2 = T_{01} - \left(\frac{V_2^2}{2c_p} \right) \rightarrow (27)$$

Considering ideal gas using relation as in Eq. 28, Eq. 29 and Eq. 30 we compute density, speed of sound and Mach number at station 2 exit.

$$\rho_2 = \frac{P_2}{RT_2} \rightarrow (28)$$

$$a_2 = \sqrt{\gamma RT_2} \rightarrow (29)$$

$$M_2 = \frac{V_2}{a_2} \rightarrow (30)$$

Using isentropic relations, we find the stagnation properties where we assume no losses. Based on this we calculate stagnation temperature and pressure using the Eq. 31 and Eq. 32.

$$T_{02} = T_{01} \rightarrow (31)$$

$$P_{02} = P_2 \left(\frac{T_{02}}{T_2} \right)^{\frac{\gamma}{\gamma-1}} \rightarrow (32)$$

From geometry of velocity triangle calculation of flow angle at exit of stator using the Eq. 33 is done.

$$\alpha_2 = \cos^{-1} \left(\frac{V_{x2}}{V_2} \right) \rightarrow (33)$$

All results have been tabulated in table 1.

2.3.2 RELATIVE ROTOR INLET CONDITION

As we have absolute conditions but there is necessity for relative frame for calculation of station 3 and also velocity triangle. So, consideration of relative velocity W is considered. The relative tangential velocity is found using Eq. 34. And from this we are able to calculate the blade angle at station 2 as in Eq. 35. Using Pythagoras theorem, we calculate actual relative velocity at station 2 as in Eq. 36.

$$W_{u2} = V_{u2} - U \rightarrow (34)$$

$$\beta_2 = \tan^{-1} \left(\frac{W_{u2}}{V_{x2}} \right) \rightarrow (35)$$

$$W_2 = \sqrt{W_{u2}^2 + V_{x2}^2} \rightarrow (36)$$

From the relative velocity we calculate the station temperature and stagnation pressure using the Eq. 37 and Eq. 38 which acts as rotor inlet conditions in the relative frame.

$$T_{02R} = T_2 + \left(\frac{W_2^2}{2c_p} \right) \rightarrow (37)$$

$$P_{02R} = P_2 \left(\frac{T_{02R}}{T_2} \right)^{\frac{\gamma}{\gamma-1}} \rightarrow (38)$$

2.3.3 ROTOR OUTLET

Using the relative frame of reference, the computed stagnation temperature and pressure is used further to calculate the rotor exit conditions. Using Eq. 39 the relative velocity isentropically is found. Using this velocity, the static temperature and real relative velocity at exit is found with rotor efficiency factor as in Eq. 40 and Eq. 41 respectively.

$$W_{3is} = \sqrt{2c_p T_{02R} \left(1 - \left(\frac{P_3}{P_{02R}} \right)^{\frac{\gamma-1}{\gamma}} \right)} \rightarrow (39)$$

$$T_{3is} = T_{02R} - \left(\frac{W_{3is}^2}{2c_p} \right) \rightarrow (40)$$

$$W_3 = \sqrt{n_r \times W_{3is}^2} \rightarrow (41)$$

Now the real relative velocity is known the static temperature, density, speed of sound and relative Mach number at station 3 is found using Eq. 42, Eq. 43, Eq. 44 and Eq. 45.

$$T_3 = T_{02R} - \left(\frac{W_3^2}{2c_p} \right) \rightarrow (42)$$

$$\rho_3 = \frac{P_3}{RT_3} \rightarrow (43)$$

$$a_3 = \sqrt{\gamma RT_3} \rightarrow (44)$$

$$M_{w3} = \frac{W_3}{a_3} \rightarrow (45)$$

Using isentropic relations, we find the stagnation properties where we assume no losses. Based on this we calculate stagnation temperature and pressure using the Eq. 46 and Eq. 47.

$$T_{03R} = T_{02R} \rightarrow (46)$$

$$P_{03} = P_3 \left(\frac{T_{03R}}{T_3} \right)^{\frac{\gamma}{\gamma-1}} \rightarrow (47)$$

From the exit velocity triangle, we find the axial component of absolute velocity. And consideration of axial flow velocity ratio as 1 for design process as in Eq. 48.

$$V_{x3} = V_{x2} \times VR_x = W_{x3} \rightarrow (48)$$

Further on, we calculate the components of velocity to get the absolute velocity component at exit of rotor which is our main aim of design process to find the actual expansion from the calculations.

$$\beta_3 = \cos^{-1} \left(\frac{W_{x3}}{W_3} \right) \rightarrow (49)$$

$$W_{u3} = W_3 \sin \beta_3 \rightarrow (50)$$

$$V_{u3} = W_{u3} + U_m \rightarrow (51)$$

$$\alpha_3 = \tan^{-1} \left(\frac{V_{u3}}{V_{x3}} \right) \rightarrow (52)$$

$$V_3 = \sqrt{V_{u3}^2 + V_{x3}^2} \rightarrow (53)$$

$$T_{03} = T_3 + \left(\frac{V_3^2}{2c_p} \right) \rightarrow (54)$$

$$P_{03} = P_3 \left(\frac{T_{03}}{T_3} \right)^{\frac{\gamma}{\gamma-1}} \rightarrow (55)$$

And finally, we arrive at enthalpy drop across the entire stage by Eq.

$$\Delta H_0 = c_p(T_{01} - T_{03}) \rightarrow (56)$$

2.3.4 COMPARISON OF ENTHALPY

The enthalpy found using the power and mass flow as in Eq. 8 is to be compared from the enthalpy found as in Eq. 56 which is done by our loop and appropriate P3 is found. This process is iterated till design criteria is not fulfilled.

The newton Raphson method iterates based on the side of solution so based the criteria shown in Fig. 3 we give the direction for advancement for solution.

$$\Delta H_T < \Delta H_{T,real} \Rightarrow P'_3 < P_3$$

$$\Delta H_T > \Delta H_{T,real} \Rightarrow P'_3 > P_3$$

$$\Delta H_T = \Delta H_{T,real} \Rightarrow OK!$$

Fig. 3: Comparison of Enthalpy for approval of design

For all iterations the step-by-step values obtained have been tabulated in table 1.

Table 1: Iterations for various properties and for different assumed values

Parameters	1st iteration	2nd iteration	3rd iteration	4th Iteration
ψ	2.5	2	1.8	1.8
ϕ	0.75	0.7	0.6	0.5
r	0.5	0.45	0.4	0.35
η_{TT}	0.84	0.85	0.86	0.87
AN2 [m ² rpm ²]	10941146.24	10288055.08	11237574.07	13405704.59
U [m/s]	296.1586785	331.1154686	349.0263498	349.0263498
P ₀₁ [Pa]	2056992.494	2056992.494	2056992.494	2056992.494
P ₁ [Pa]	2026500	2026500	2026500	2026500
T ₀₁ [K]	1679.211013	1679.211013	1679.211013	1679.211013
T ₁ [K]	1673	1673	1673	1673
V ₁ [m/s]	173.39788	178.7872898	159.5559113	131.0255048
V _{x1} [m/s]	173.39788	178.7872898	159.5559113	131.0255048
α_1 [Degree]	0	0	0	0
M ₁	0.15	0.15	0.15	0.15
P ₀₂ [Pa]	1964747.411	1961515.168	1958179.909	1954202.055
P ₂ [Pa]	1502372.052	1479445.234	1456195.59	1428996.989
T ₀₂ [K]	1679.211013	1679.211013	1679.211013	1679.211013
T ₂ [K]	1571.057232	1565.713618	1560.230794	1553.73253
V ₂ [m/s]	500.2022583	512.4101726	524.6409413	538.7774681
V _{x2} [m/s]	222.1190089	231.780828	209.4158099	174.5131749
V _{u2} [m/s]	448.1801481	456.9921583	481.0334041	509.7316078

α_2 [Degree]	63.63688952	63.1064344	66.47430779	71.10070045
M_2	0.645926163	0.662818787	0.679831036	0.699607613
P_{02R} [Pa]	1626763.73	1597340.922	1558430.684	1521338.131
T_{02R} [K]	1602.373724	1595.785147	1586.720378	1578.060868
W_2 [m/s]	269.1605122	263.7561246	247.5496795	237.2362286
W_{x2} [m/s]	72295.35985	69441.41656	61148.83676	56120.3229
W_{u2} [m/s]	152.0214696	125.8766897	132.0070543	160.705258
β_2 [Degree]	34.3883041	28.50572106	32.22563335	42.64127415
M_{w2}	0.347575034	0.341176901	0.32077549	0.308053476
P_{03R} [Pa]	1541485.745	1525691.007	1499400.823	1472070.083
T_{03R} [K]	1602.373724	1595.785147	1586.720378	1578.060868
W_3 [m/s]	628.9056061	584.2929326	538.6181314	499.0496272
W_{x3} [m/s]	222.1190089	231.780828	209.4158099	174.5131749
W_{u3} [m/s]	588.3752266	536.3542475	496.2403753	467.5421716
β_3 [Degree]	69.31785094	66.62883269	67.12002278	69.5315821
Turning ($\beta_2 + \beta_3$) [Degree]	103.706155	95.13455375	99.34565612	112.1728563
M_{w3}	0.850820041	0.785865122	0.721177411	0.666129225
P_{03R} [Pa]	1148816.885	1156084.803	1162550.689	1166812.988
P_3 [Pa]	978244.1037	1031854.971	1075992.65	1107264.599
T_{03} [K]	1489.641131	1489.641131	1489.641131	1489.641131
T_3 [K]	1431.403162	1448.210527	1461.316102	1470.404957
V_3 [m/s]	367.0522648	309.5889349	255.982325	210.9522416
V_{x3} [m/s]	222.1190089	231.780828	209.4158099	174.5131749
V_{u3} [m/s]	292.2165481	205.2387789	147.2140255	118.5158218
α_3 [Degree]	52.76088682	41.52445414	35.10624989	34.18130788
M_3	0.3	0.3	0.3	0.3
Height2 (h_2) [m]	0.171087186	0.148412206	0.157766437	0.1921196
Height3 (h_3) [m]	0.239396451	0.196819998	0.199977138	0.234645523
h_2/h_3	1.399265811	1.326171235	1.267551844	1.221351298
R_{T2} [m]	1.028245946	1.128179374	1.189868595	1.207045177
R_{T3} [m]	1.062400578	1.15238327	1.210973946	1.228308138
R_{H2} [m]	0.857158759	0.979767168	1.032102158	1.014925577

R_{H3} [m]	0.823004127	0.955563272	1.010996808	0.993662615
ε [Degree]	27.19224491	22.76798561	18.99729958	15.89832571

From the table 1 we observe that at iteration 4 the results are closest to the design conditions and hence we use them for our calculations for further design.

2.4 VELOCITY TRIANGLES

Based on the calculation at stations 2 and station 3 along with the relative frame of reference the velocity triangle is plotted as in Fig. 4. The velocity triangle plots the blade speed (U), absolute velocity (V) and relative velocity (W) with flow (α) and blade angles (β) at stations 2 and station 3.

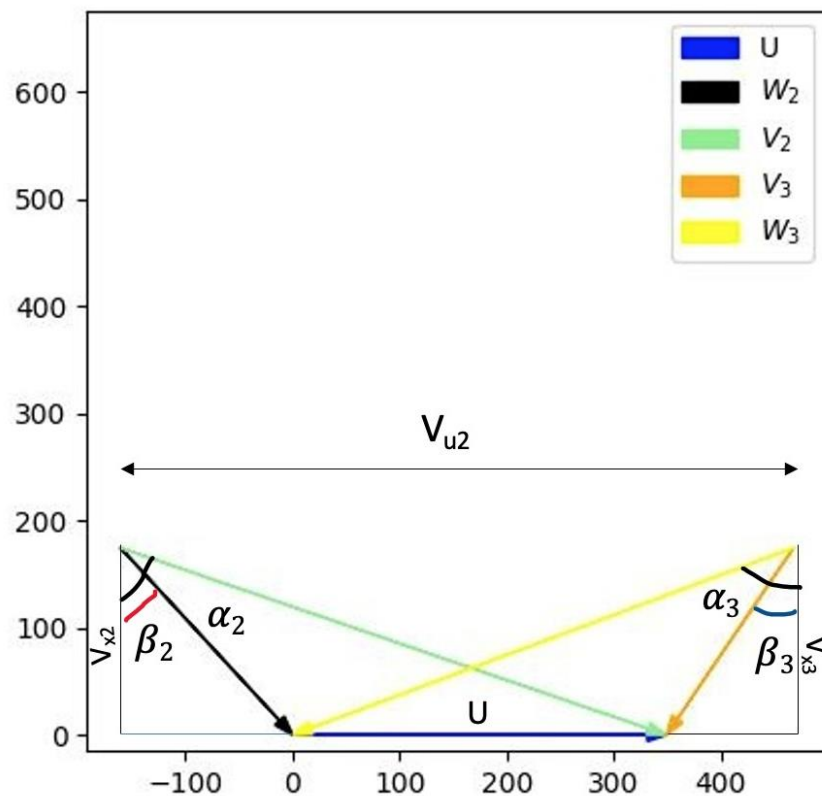


Fig. 4: Velocity triangle for both station 2 and 3

Table 2: Velocity triangle parameters data

Parameter	Station 2	Station 3
U (Blade Speed) [m/s]	349.0263498	349.0263498
V (Absolute Velocity) [m/s]	538.7774681	210.9522416
W (Relative Velocity) [m/s]	237.2362286	499.0496272

α (Flow Angle) [Degree]	71.10070045	34.18130788
β (Blade Angle) [Degree]	42.64127415	69.5315821

2.5 H-S DIAGRAM

The H-S plot as shown in Fig. 5 and the results have been tabulated in Table 3. This represents the change in enthalpy at different stations and their isentropic relation with different entropy cycle. This helps engineers to understand the need for thermal conditions, work production and phase change of the flow and many more parameters. The entropy is assumed randomly. Using the table 3 we plot the H-S diagram as in Fig. 5.

Table 3: Enthalpy-Entropy results table

Parameter	Enthalpy [J/kg]
H1	1942338.28964053
h1	1933754.4481835
h2	1797197.70955331
h2s	1781070.9784325
H2	1942338.28964053
H2r	1825338.22363202
h3	1700812.9584117
h3s	1686976.81783167
H3	1723063.38252845
h3ss	1664255.80024295
H3ss	1708756.64847644

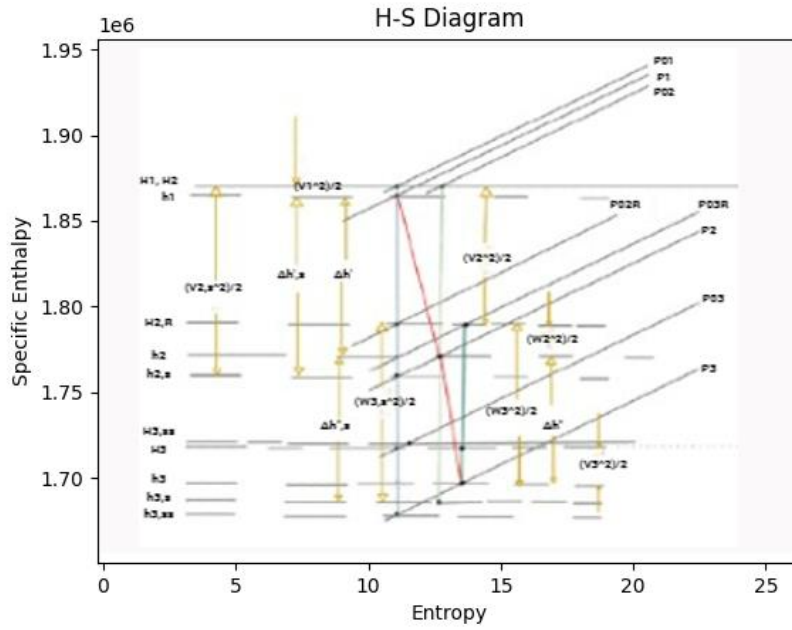


Fig. 5: H-S Plot for 1st Stage of Turbine

2.6 ANNULUS SIZING

Annulus sizing refers to the diameter or radius of the blade cylinder. As there is an expansion process we need to take of the flow as there might losses. We consider shrouded condition where the assumption is that end wall contour control ε at the tip and hub is equal which is a good approximation to make for easier calculations. We perform the height calculations at station 2 and station and results have been tabulated in table 1.

2.6.1 SIZING AT STATION 2

The area at station 2 is calculated with the conservation of mass Eq. 57. And found the height using Eq. 58. Using the Eq. 59 we find the mean radius using mean blade speed with number of rotations as N.

$$A_2 = \frac{\dot{m}}{\rho_2 V_{x2}} \rightarrow (57)$$

$$h_2 = \frac{A_2}{\pi D_{m2}} \rightarrow (58)$$

$$R_m = \frac{60 U_m}{2 \pi N} = 1.11 m \rightarrow (59)$$

The tip and hub radius are found using Eq. 60 and Eq. 61 respectively at station 2.

$$R_{T2} = R_m + \frac{h_2}{2} \rightarrow (60)$$

$$R_{h2} = R_m - \frac{h_2}{2} \rightarrow (61)$$

2.6.2 SIZING AT STATION 3

The area at station 3 is calculated with the conservation of mass Eq. 62. And found the height using Eq. 63.

$$A_3 = \frac{\dot{m}}{\rho_3 V_{x3}} \rightarrow (62)$$

$$h_3 = \frac{A_3}{\pi D_{m3}} \rightarrow (63)$$

The tip and hub radius are found using Eq. 64 and Eq. 65 respectively at station 3.

$$R_{T3} = R_m + \frac{h_3}{2} \rightarrow (64)$$

$$R_{h3} = R_m - \frac{h_3}{2} \rightarrow (65)$$

All values have been tabulated in table 1.

2.6.3 SIZING AT STATION 1

Considering the area found at station 1 is same as the area at station 2 as we assume the area ratio between station at 1 and 2 as 1 i.e., $A_{12, ratio} = 1$ shown in Eq. 66.

$$A_1 = A_2 \times A_{12, ratio} = 1.34 \text{ m}^2 \rightarrow (66)$$

The Mach number, static pressure and temperature at station 1 is known hence the loop to find M1 is not a good approach for calculation.

2.6.4 END WALL CONTOUR CONTROL (E)

Assuming the aspect ratio as explained in the section 2.1, the axial chord is calculated and the end wall angle epsilon is found using the Eq. 67.

$$\varepsilon = \tan^{-1} \left(\frac{h_3 - h_2}{c_x} \right) = 15.89 [\text{degree}] \rightarrow (67)$$

2.6.5 AN2 VALUE CALCULATION

Using Eq. 68 we calculate the AN2 and observe it with desired range as in table 3.

$$AN^2 = \frac{A_3 + A_2}{2} \times N^2 = 1.3e^7 \rightarrow (68)$$

2.7 DESIGN CONSTRAINTS

As the discussions for design constraints is made throughout then defining these constraints is a very important thing to compare with the results obtained. The table 4 interprets the range of values for design constraints and obtained values from the calculations.

Table 4: Comparison of design control parameters and obtained results

Design Control parameter	Design Range	Obtained Results
M_2 [$r = 0.35$ & $\Pi = 2-3$]	0.7 – 0.85	0.699
β_2 [Degree]	< 47.5	42.641
M_{w2}	<0.5	0.308
M_{w3} [$r = 0.35$ & $\Pi = 2-3$]	0.65-0.8	0.666
β_3 [Degree]	<75	69.531
$\Delta\beta$ [Degree]	110-120	112.173
M_3	0.3	0.3 (Assumed)
α_3 [Degree]	30-35 (if losses), else <30	34.181
h_3 / h_2	<1.1 – 1.2	1.218
AN^2 [m^2rpm^2]	< $3e^7$	$1.3e^7$
ε [Degree]	<15	15.89

The table 4 gives a very good opinion of the design as the range very closely matched with the design range and is approved for next step of rotor design as in section 2.

3. ROTOR BLADE DESIGN

The rotor blade design starts with steps of few assumptions which are important for further calculation like blade characteristics having information about airfoil shape and structure. Also, calculation of number of blades is made from these assumptions. Parablade software is used to design the rotor blade based on the values obtained from these calculations.

3.1 INPUT DATA ASSUMPTIONS

1. Aspect ratio (AR):

Aspect ratio is defined as the ratio of span (b) to chord length (\bar{c}) as in Eq. 69. Since we are unaware of chord and aspect ratio, we assume aspect ratio based on certain conditions.

$$AR = \frac{b}{\bar{c}} = 1 \rightarrow (69)$$

Aspect ratio for high pressure vary from 1 – 1.5 based on various resources. And we assume aspect ratio as 1 which gives us best design values.

2. Stagger angle (ξ):

Stagger angle defines as the angle between the chord and direction of fluid flow. We choose the stagger angle by using the plot of β_2 and β_3 as shown in Fig. 6. We find stagger angle for β_2 and β_3 obtained as 42.64127415 and 69.5315821 degrees respectively we obtain stagger angle around 39 degrees.

$$\xi = 39 [Degrees]$$

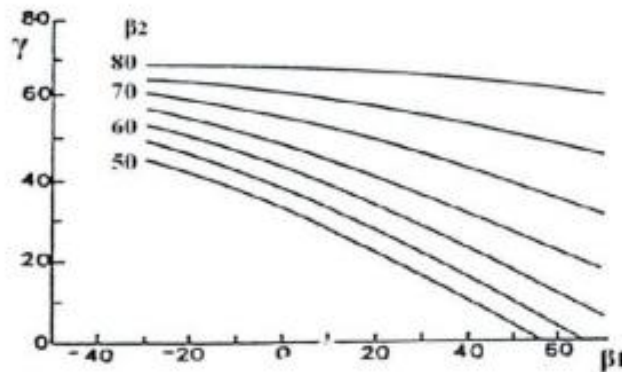


Fig. 6: Stagger Angle correlation [Kacker and Okapuu, 1982]

3. Zweifel Coefficient (ψ)

This coefficient is given as 1 in this case. It is generally referred for optimal pitch to chord ratio and describes the tangential aerodynamic force generated by blade as a function of surface area. Previously it used to be below 1 but recent times these losses are recovered and hence assumed 1 for design.

$$\psi = 1$$

3.2 DESIGN PROCEDURE & CALCULATIONS

1. Chord (\bar{c})

We need to design blades which are made of airfoils which has both pressure and suction side to get little lift for easy rotation. We get chord length by using Eq. 70 from the values of height at station 2. And using Eq. 71 we compute the axial component of the chord using the stagger angle.

$$\bar{c} = \frac{h_2}{AR} = 0.192m \rightarrow (70)$$

$$c_x = \bar{c} \times \cos \xi = 0.149m \rightarrow (71)$$

2. Pitch (s):

Pitch is the distance between the leading edge of the blades in cascade view which is represented by s and is found using the Eq. 72.

$$s = \frac{Z \times c_x}{2 \cos^2 \beta_3 (\tan \beta_2 + \tan \beta_3)} = 1.113m \rightarrow (72)$$

3. Number of blades (NoB):

Important point of observation is the design for number of blades. The number of blades is found from the Eq. 73 using the parameters of pitch and mean diameter.

$$No. of Blades = \frac{\pi D_{m2}}{s} = 42 \rightarrow (73)$$

4. Thickness distribution and Thickness to chord ratio (t_{max}/\bar{c}):

Blade thickness varies in the range of 0.15 to 0.25 times the chord. Using the plot having variation t/c ratio and turning angle, using this we obtain our thickness to chord ratio.

$$\frac{t_{\max}}{c} \approx 0.25$$

5. Leading and trailing edge radius (R_{LE}/R_{TE}):

For construction we need to define the radius of inlet and exit of airfoil. The leading edge has a tendency of flow separation and force the flow to stall hence for better tolerance which lies between 0.025 to 0.1 of the pitch (s). As we have less Mach number, we can provide a greater leading-edge radius as the flow stalling tendency is lesser. And for trailing edge cooling is a major factor to be chosen and hence we keep it above 0.5mm.

Hence, we consider,

$$R_{LE} = 5\% \times 1.113 = 0.0556 \text{ m}$$

$$R_{TE} = 0.0007 \text{ m}$$

3.3 MAIN BLADE PARAMETERS

The main blade parameters which are necessary to plot an airfoil based on some assumptions and calculations as done in section 2.1 and 2.2. All the results obtained from it has been tabulated in table 5. These parameters are useful for plotting the blade and analysing for the flow.

Table 5: Main Blade Parameters

Parameter	Values
α_2 (Flow Angle) [Degree]	71.10
β_2 (Blade Angle) [Degree]	42.64
α_3 (Flow Angle) [Degree]	34.18
β_3 (Blade Angle) [Degree]	69.53
Aspect Ratio (AR)	1
Stagger angle (ξ) [Degree]	39
Zweifel Coefficient (ψ)	1
Chord (\bar{c}) [m]	0.192
Pitch (s) [m]	0.149
Number of Blades (NoB)	42
Thickness to chord ratio (t_{\max}/\bar{c})	0.25

Leading Edge Radius (R_{LE})	0.0556
Trailing Edge Radius (R_{TE})	0.0007
Axial Chord c_x [m]	0.149
Spacing (s) in [m]	1.113
Stagger angle [Degree]	-39.0
theta_in [Degree]	42.64
theta_out [Degree]	-69.53
dist_in [m]	0.60
dist_out [m]	0.40
radius_in [m]	0.0556
radius_out [m]	0.0046
Airfoil Thickness variation	
thickness_upper_1	0.15
thickness_upper_2	0.20
thickness_upper_3	0.13
thickness_upper_4	0.07
thickness_upper_5	0.03
thickness_upper_6	0.03
thickness_lower_1	0.12
thickness_lower_2	0.17
thickness_lower_3	0.10
thickness_lower_4	0.07
thickness_lower_5	0.03
thickness_lower_6	0.03

4. ROTOR BLADE CONSTRUCTION AND CFD EVALUATION

4.1 BLADE PASSAGE GEOMETRY

Based on the design calculation for the profile the values are inputted in the parablade. The parablade executes the python code based on the parameters as in rotor design and executes an airfoil with blade passage and its profile as shown in Fig. 7 and Fig. 8.

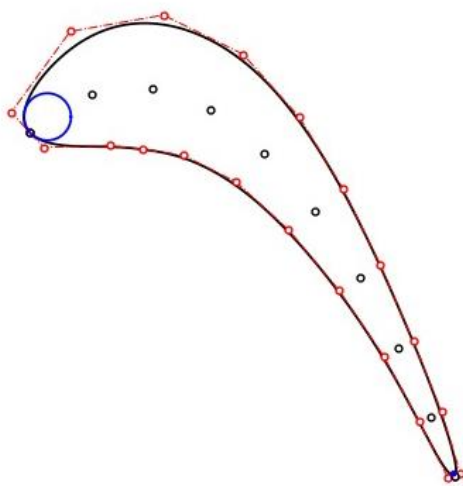


Fig. 7 Blade Profile Diagram

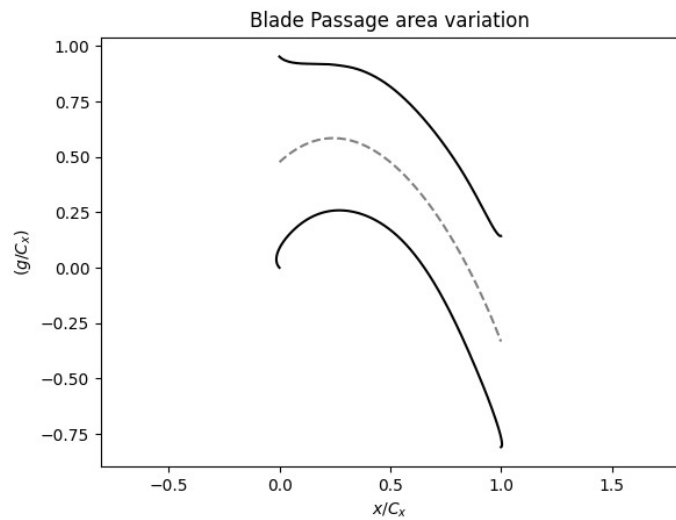


Fig. 8 Blade passage area variation

4.2 EVALUATION OF PROFILE CURVATURE AND PASSAGE AREA

The evaluation of profile is done by the reaction 2D file which takes the input from table 5. These values are inputted and using the gmsh software a mesh is created for CFD evaluation.

The stagger angle, theta inlet and exit, axial chord and other values calculated already are inputted. But to optimize the airfoil based on thickness we change when the results turn out with shocks or variation in flow. In our case with high pressure turbine the Mach number is below 1 and formation of shocks is not occurring. Hence the required thickness is kept constant without fluctuations.

This part of code executes the results with the variation of blade thickness with reference along u , curvature κ along u and also the cascading view as shown in Fig. 9, Fig. 10 and Fig. 11 respectively.

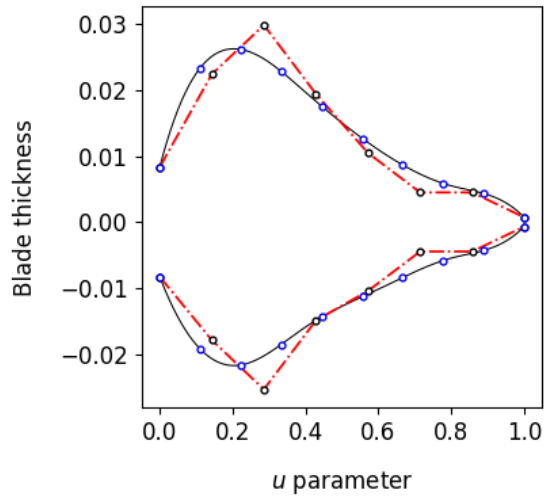


Fig. 9: Blade thickness variation along u

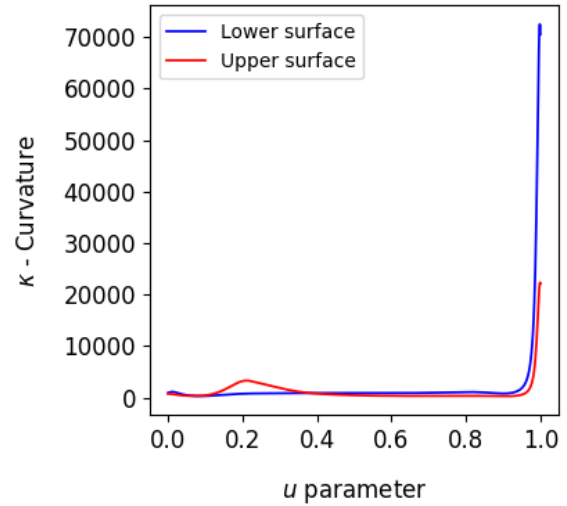


Fig. 10: Curvature κ along u



Fig. 11: Cascading View of turbine rotor blades of stage 1

4.3 CFD EVALUATION

4.3.1 MESH GENERATION

With the 2D profile of blade using GMSH a mesh is generated. This mesh of blade profile is used further for CFD evaluation using SU2 solver. The Fig. 12 represents the blade profile generated using GMSH.

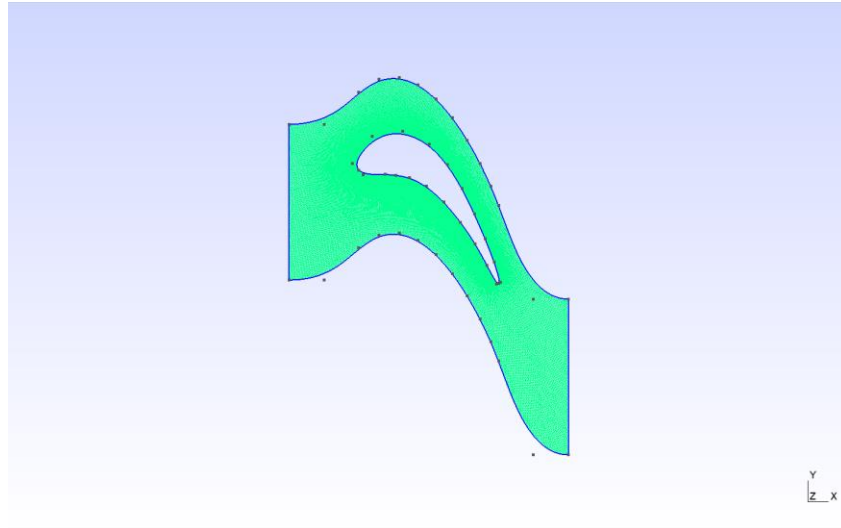


Fig. 12: Blade profile generated using GMSH

4.3.2 CFD SETTING

To perform various CFD settings need to be changed in the SU2 software to evaluate the blade based on the requirement of the flow.

In this case we change parameters as shown in Table 6.

Table 6: SU2 CFD solver configuration data

Parameter	Value
Solver	RANS
Convergence Numerical Method	Scalar Upwind
Reynold's Number (Re)	1e5
Mach Number	0.308
Specific Constant (γ)	1.33
Freestream Temperature [K]	288
Freestream Pressure [Pa]	101325
REF_LENGTH [M]	0.149
T01 [K]	1578.061
P01 [Pa]	1521338.131
lx [m]	0.735
ly [m]	0.677
Pitch [m]	-0.166

Iterations	10000
Error	1e-4
Time Decrement Flow Method	Euler Implicit

4.3.3 CFD CONVERGENCE

The simulations are performed for investigating the Coefficient of drag for the error as mentioned in table 6. A steady RANS simulation is performed and converged. The convergence completion is shown in Fig. 13.

1806	-8.784127	-7.115977	-6.942294	-4.241602
1807	-8.786558	-7.118162	-6.944529	-4.243496
1808	-8.788992	-7.120344	-6.946765	-4.245402
1809	-8.791426	-7.122524	-6.949001	-4.247322
1810	-8.793863	-7.124703	-6.951238	-4.249257
1811	-8.796301	-7.126880	-6.953473	-4.251212
1812	-8.798740	-7.129057	-6.955708	-4.253186
1813	-8.801181	-7.131234	-6.957941	-4.255183


```

----- Solver Exit -----
All convergence criteria satisfied.
+-----+
| Convergence Field | Value | Criterion | Converged |
+-----+
| Cauchy[CD] | 9.99542e-11 | < 1e-10 | Yes |
+-----+
+-----+
| File Writing Summary | Filename |
+-----+
| Paraview | flow.vtu |
| CSV file | surface_flow.csv |
+-----+

```

Fig. 13: Cauchy CD Convergence

4.4 ISENTROPIC STATIC PRESSURE DISTRIBUTION

From the CFD evaluation the static pressure distribution about the aerofoil on pressure and suction side has been plotted as in Fig. 14.

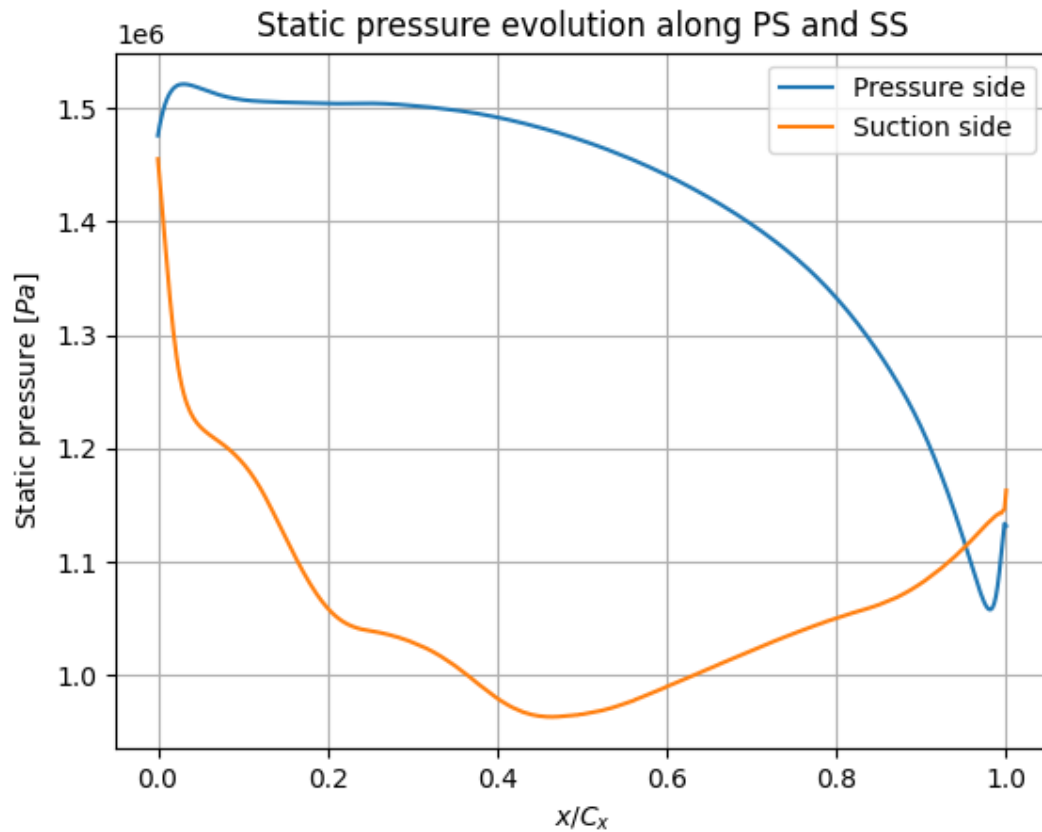


Fig. 14: Static pressure variation along the blade

The plot shows the variation of static pressure which shows the pressure side has greater static pressure but along the airfoil it keeps decreasing while it is inverse for the suction side where it first decreases and then steeply increases which allows it from lift in downward direction allowing the blade to create a lift in direction of the blade rotation direction to receive a greater velocity. Little variation maybe caused due to losses occurred while flow moves through the blade profile either as profile loss or secondary loss.

4.5 COLOURMAPS OF CFD ANALYSIS

The Fig. 15, Fig.16, Fig. 17 and Fig. 18 shows the colourmaps along the blade profile and surrounding variation of Mach, pressure, enthalpy and entropy along the profile. From the colourmaps we observe that the mach number on the suction side is higher than on pressure side, which is inversely proportional to the pressure which is less on suction side than on pressure side. Specific Enthalpy is almost constant but near the wake region where flow

separates there is a drop which is similar in case of entropy as in wake region pressure drop occurs and even Mach number is comparatively lower allowing an opposite force against lift.

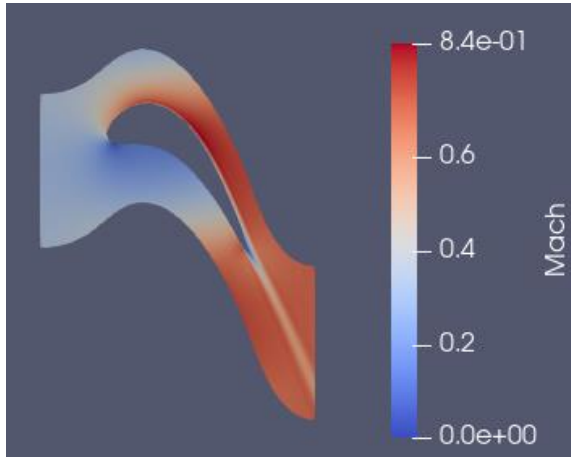


Fig. 15: Mach variation along the blade

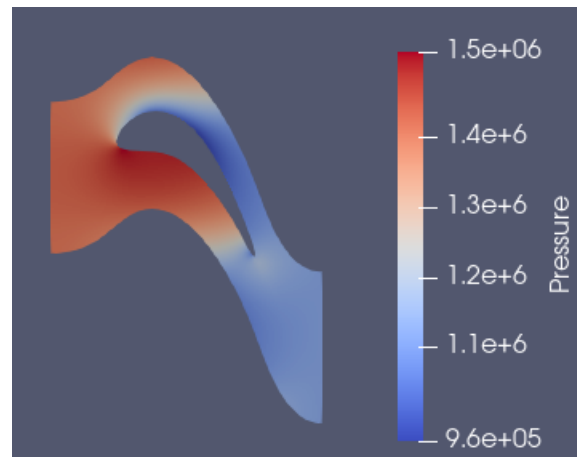


Fig. 16: Pressure variation along the blade

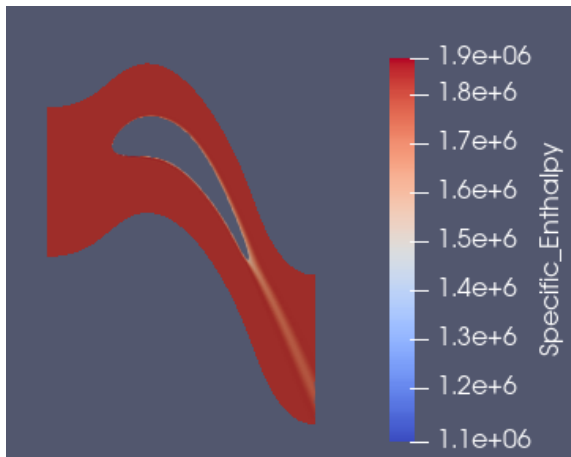


Fig. 17: Specific Enthalpy variation

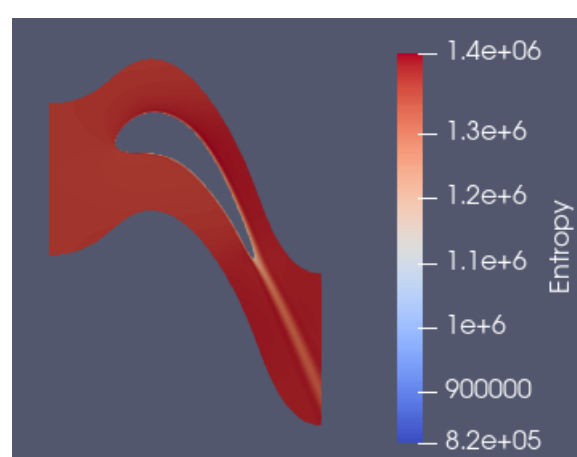


Fig. 18: Entropy variation

In these plots there is a formation of boundary layer which is attached till the end of the flow which is desirable as flow separation happens after 90 degrees as a turbulent boundary layer. This leads to some loss of flow velocity in compensation of flow separation which is affordable for the blade design for a high-pressure turbine. Also, it is clearly visible as the inlet flow angle is zero considered the blades have stagnation points at entry itself. The Mach number does not reach unity which does not allow formation of shocks as desired for design of blades.

4.6 VELOCITY PROFILE HIGHLIGHT THE MOMENTUM DEFICIT IN WAKE

The wake region has loss of lift due to large pressure drop caused by flow separation. From Bernoulli's equation we can say that pressure drop is directly proportional to momentum loss. The compensation of pressure drop is compensated by velocity but due to flow separation it does not fully compensate for the pressure loss due to which a huge drop is visible from the Fig. 19 in the wake region plotted by plotting over a line in paraview software at the wake region.

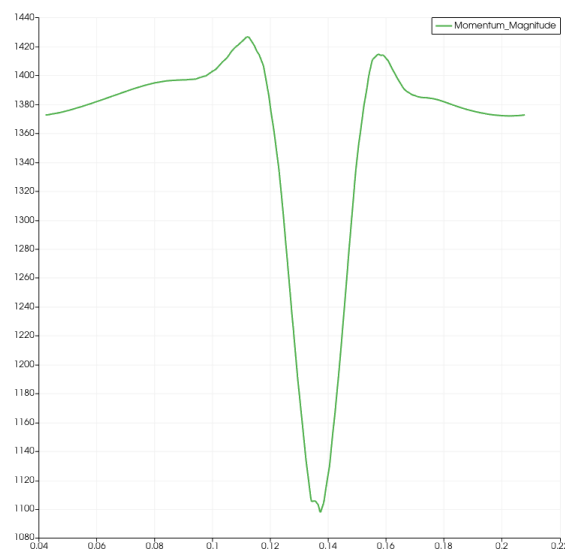


Fig. 19: Momentum variation in the wake

4.7 CFD PREDICTION RESULT:

Paraview software has many options to perform in them is to plot over a line for different parameters. To view various parameters at half a chord downstream the rotor trailing edge. We plot the variation of stagnation pressure along the pitch wise direction in Fig. 20. The Fig. 21 represents the Mach number variation along the pitch wise distribution.

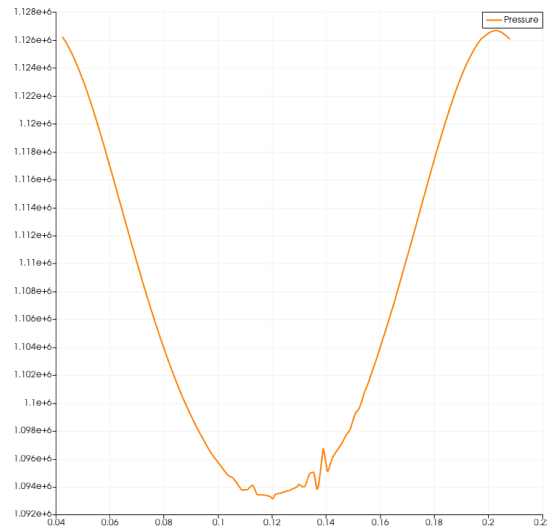


Fig. 20: Stagnation pressure Distribution along the pitch

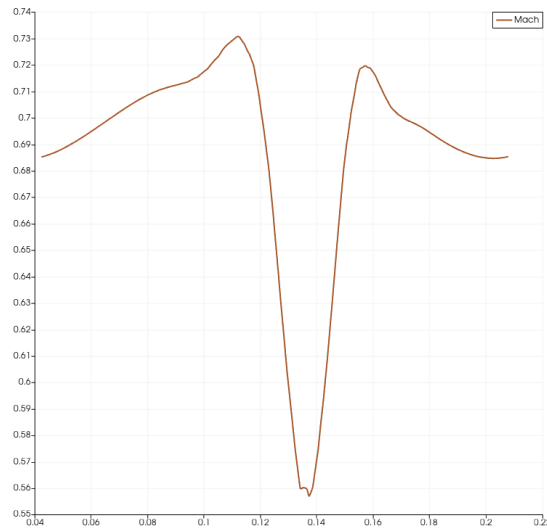


Fig. 21: Mach Distribution along the pitch

From the plots we observe that there is a drop in stagnation pressure which is collective effort of static pressure and velocity (Mach). As the flow separates the lift generation take place in opposition as forcing to move the blades in opposite direction which reduces speed of blade forming a problem as a loss due to wake. But as we move towards end the flow returns to its original path.

The Flow angle is determined by using the plots of momentum in x and y -direction as difference which provides a percentage. This percentage times maximum momentum magnitude gives the total momentum loss. Flow angle is determined by Eq. 74.

$$\alpha = \cos^{-1} \left(\frac{M_x}{M_{Loss}} \right) = 62.5135^\circ \rightarrow (74)$$

5. CONCLUSION

The turbine design was focused on being highly efficient with maximum power output for extracting work from the turbine. A set of iterations were performed to fit the engine based on the design requirements. Maximizing efficiency helped to take care of friction loss and leakage due to secondary losses and profile losses to some extent. The unshrouded design would have helped to decrease tip losses as it creates turbulent boundary layers which will hold the flow without separation from the blades. Since the engine is used for high pressure stage the power extracted is high enough and cooling has been taken care of. This is the first stage of high pressure implying to increase in losses due to other effects other than shock formation. The design takes care of aerofoil design which is of less importance as the flow is laminar but it should handle the high pressure and high camber thickness enough for cooling effects. The CFD results show the formation of a small wake region which is not to an extent of stall or other catastrophic behaviour. The entire design is done for a cascade view. The minimum input known has been utilized to get very good results for 1st stage of turbine design.